



ELSEVIER

Contents lists available at ScienceDirect

Virology

journal homepage: www.elsevier.com/locate/yviro

Conserved amino acids within the N-terminus of the West Nile virus NS4A protein contribute to virus replication, protein stability and membrane proliferation

R.L. Ambrose¹, J.M. Mackenzie*

Department of Microbiology and Immunology, University of Melbourne, Peter Doherty Institute for Infection and Immunity, Melbourne, VIC, Australia

ARTICLE INFO

Article history:

Received 27 January 2015

Returned to author for revisions

16 February 2015

Accepted 19 February 2015

Available online 13 March 2015

Keywords:

West Nile virus

Virus replication

Intracellular membrane proliferation

Replication complex

ABSTRACT

The West Nile virus strain Kunjin virus (WNV_{KUN}) NS4A protein is a multifunctional protein involved in many aspects of the virus life-cycle and is a major component of the WNV_{KUN} replication complex (RC). Previously we identified a conserved region in the C-terminus of NS4A regulating proteolytic processing and RC assembly, and now investigate key conserved residues in the N-terminus of NS4A and their contribution to WNV_{KUN} replication. Mutation of P13 completely ablated replication, whereas, mutation of P48 and D49, near the first transmembrane helix, and G66 within the helix, showed variable defects in replication, virion secretion and membrane proliferation. Intriguingly, the P48 and G66 NS4A mutants resulted in specific proteasome depletion of NS4A that could in part be rescued with a proteasome inhibitor. Our results suggest that the N-terminus of NS4A contributes to correct folding and stability, essential for facilitating the essential roles of NS4A during replication.

© 2015 Elsevier Inc. All rights reserved.

Introduction

West Nile virus strain Kunjin (WNV_{KUN}) is an enveloped, positive sense RNA virus belonging to the *Flaviviridae* family, within the *Flavivirus* genus. These viruses are typically vector-borne, and are transmitted between their reservoir bird host and other species by mosquitoes or ticks. Intracellular replication of WNV_{KUN} and other *Flaviviruses* occurs within the cytoplasm of infected cells, and is typically associated with extensive proliferation and re-organisation of intracellular membranes (Mackenzie, 2005). These membranes have two proposed roles during replication; to protect replicative components from detection by immune effectors, and to spatially segregate viral RNA transcription from polypeptide expression and processing, thus allowing more effective replication. WNV_{KUN} induces the formation of two distinct membrane compartments: the vesicle packets (VP), which enclose the replicating RNA intermediates and components of the replication complex (RC) (NS1, NS2A, NS3, NS4A and NS5), and the convoluted membrane (CM)/paracrystalline array (PC) structures, which are the proposed sites of viral protein translation and proteolytic processing by the NS2B-3 protease (Mackenzie et al., 2001; Westaway et al., 1997b). The source of these membranes is

thought to be the endoplasmic reticulum (ER), which is also the site of virion assembly (Gillespie et al., 2010; Mackenzie and Westaway, 2001).

The small, hydrophobic proteins encoded by the *Flaviviridae* are proposed to aid in the proliferation of intracellular membranes. An example of this is NS4B from the Hepacivirus Hepatitis C virus, which when individually expressed induces proliferation of the ER into membranous webs, characteristic of those formed in infection (Egger et al., 2002). Similarly, expression of the small hydrophobic protein NS4A of WNV_{KUN} and dengue virus (DENV) causes distinct membrane proliferations similar to the CM/PC structures observed during replication (Miller et al., 2007; Roosendaal et al., 2006). Flavivirus NS4A is a 16 kDa, ER localised non-structural protein that has three transmembrane helices, a membrane associated region and a cytoplasmic N-terminus (Mackenzie et al., 1998; Miller et al., 2007). In addition to its role in membrane proliferation, NS4A is also predicted to form part of the WNV_{KUN} RC, suggested from studies which have shown interactions with the replicative intermediates dsRNA, NS1, NS2A and NS5 as well as self-oligomerisation (Chu and Westaway, 1992; Mackenzie et al., 1998). Based on topology studies, it has been proposed that NS4A acts to anchor the complex to the VP membranes by its transmembrane regions, whilst interacting with the replicative components via its cytoplasmic N-terminus (Westaway et al., 2002). Recent reports with DENV NS4A have identified an amphipathic helix within the first 20 residues of the cytoplasmic domain, which when mutated reduced oligomerisation and

* Corresponding author. Tel.: +61 3 9035 8376; fax: +61 3 8347 1540.

E-mail address: jason.mackenzie@unimelb.edu.au (J.M. Mackenzie).¹ Present address: CSIRO-AAHL, Geelong, VIC, Australia.

intracellular replication (Stern et al., 2013). Additionally, this cytoplasmic region of NS4A has also been proposed to interact with the cellular scaffolding protein vimentin (Teo and Chu, 2014), which is required for efficient replication. We and others have also shown that NS4A plays a vital role in the regulation of cellular processes, specifically stress responses (unfolded protein response and autophagy signalling) and innate immune pathways (Ambrose and Mackenzie, 2011b; Lin et al., 2008; Liu et al., 2005; McLean et al., 2011; Munoz-Jordan et al., 2003).

Our previous work in this field has interrogated the role of conserved residues of WNV_{KUN} NS4A in its functions during intracellular replication. Across the Flavivirus genus, NS4A is highly conserved, particularly within the transmembrane regions. We identified a conserved motif in the cytoplasmic loop between the last two transmembrane helices (Pro–Glu–Pro–Glu) which is vital for WNV_{KUN} replication and virion production (Ambrose and Mackenzie, 2011a). Mutation of these residues resulted in loss of correct proteolytic processing of NS4A, and associations with RC components, which we proposed was the reason for replication attenuation. We were thus interested in investigating other conserved regions within the N-terminal portion of NS4A and whether they contributed to the function(s) of NS4A during replication. A highly conserved proline in the first 20 amino acids was essential, as alanine substitution completely ablated all protein and virus production. Two mutations (P48A and G66A) were highly attenuated and resulted in a specific, proteasome-mediated depletion of the mutant NS4A proteins. This loss of expression also resulted in inefficient replication and decreased proliferation of a subset of virus-induced membranes. However, restoration of NS4A levels by inhibition of the proteasome induced expansion of the ER, which we attributed to increased expression of the membrane-inducing NS4A.

Results

N-terminal mutations differentially impair virus replication and virion secretion

Previously we identified a conserved motif (Pro–Glu–Pro–Glu) in the C-terminal cytoplasmic loop of NS4A, that is critical for proteolytic processing at the NS4A-2K site and formation of the WNV_{KUN} RC (Ambrose and Mackenzie, 2011a). Extending those studies, we were interested in investigating the importance of other conserved domains in NS4A that function during WNV_{KUN} replication. Based upon our previously published alignment (Ambrose and Mackenzie, 2011a), see also Supplementary Fig. 1, we identified 4 additional residues of interest in the N-terminal half of NS4A; namely Pro13 in the cytoplasmic region, Pro48 and Asp49 at the junction between the cytoplasmic and first transmembrane helix regions, and a completely conserved glycine (Gly66) in the middle of the first transmembrane helix. We generated point mutations in the WNV_{KUN} infectious clone, FLSDX, to change each residue separately to alanine (and to serine for Gly66), then electroporated the transcribed RNA from each mutation into Vero cells. RNA, protein lysates and t.c.f. samples were collected and analysed at 24, 48 and 72 h.p.e. As shown in Fig. 1, the mutations had variable effects on RNA replication, viral protein synthesis and virion secretion. The P13A mutation was a lethal mutation, as demonstrated by the absence of viral proteins or infectious virions at all timepoints assayed. Low levels of WNV_{KUN} genomic RNA were detectable, however, as these did not increase over the timecourse (Fig. 1A–C). P48A was severely attenuated, with significant decreases in genome replication (Fig. 1A–C), viral protein production (Fig. 1D–F) and virion secretion (Fig. 1G) across all timepoints assayed. In comparison, the neighbouring D49A mutation only caused mild defects in replication, most notably at 24 h.p.e., and by later timepoints showed comparable levels of RNA, protein and virus production

to the WT samples. The glycine mutations (G66A and G66S) also showed variable effects on replication; the alanine mutation was highly attenuated, with reduced RNA, protein and virus production, whilst the more conservative mutation to serine showed only moderate effects similar to the D49A mutation. The plaque sizes of secreted virions (Fig. 1H) also reflect these effects, with the more attenuated P48A and G66A showing dramatically smaller plaques compared to the milder effects of the D49A and G66S mutations.

However, of most interest was the dramatic difference in NS4A protein levels between the various mutants. This was particularly apparent at 48 h.p.e. (Fig. 1E); compared to the modest decreases in NS5 levels in the P48A and G66A samples, the levels of NS4A were markedly reduced whilst the less attenuated mutants showed a similar NS4A and NS5 levels. This is especially significant as all WNV_{KUN} proteins are translated from a single transcript, and thus should all be expressed at a 1:1 ratio. However, when analysed by densitometry (Fig. 1E and F), we observed that in the more attenuated mutants, the ratio of NS4A:NS5 (using actin as the loading control) was drastically reduced (0.27 for the P48A mutant), although it should be noted that these are arbitrary values derived from the western blots without standards. These results suggest that the replication defects observed in these mutants could be attributed to decreased NS4A levels during early stages of replication.

N-terminal mutations partially affect replication but do not prevent replication complex formation

To assess the effect of the Ala/Ser mutations (and associated decreases in NS4A protein levels) on intracellular events of replication, we analysed the associations of NS4A with the RC components NS1 (Fig. 2) and dsRNA (Fig. 3) by immunofluorescence at 48 h.p.e. in all mutants. As predicted from the qPCR and western data, no staining of any viral component was observed in the P13A null mutant (data not shown), and as such, this sample was excluded from further analysis. The FLSDX WT-electroporated cells showed typical NS4A staining (Fig. 2a), which co-localised with NS1 (Fig. 2b and c; Pearson's coefficient: $R_r=0.759$) in a reticular pattern, with some larger cytoplasmic foci. The D49A and G66S mutants (Fig. 2g–i and m–o) showed a similar phenotype and equal levels of co-localisation with NS1, which correlated with the near-WT levels of NS4A and replication at this timepoint (Pearson's coefficient: $R_r=0.860$ and $R_r=0.816$, respectively). As we had previously shown that NS4A is required for RC formation, we hypothesised that the reduced expression levels of mutant NS4A in the P48A and G66A samples would also result in loss of RC associations with NS1. Both NS4A and NS1 staining in these samples (Fig. 2d–f and j–l) were more diffuse and less reticular compared to WT, however, colocalisation of NS4A with NS1 was reduced but still apparent (Pearson's coefficient: $R_r=0.683$ and 0.698 , respectively). When we investigated the associations of NS4A and dsRNA (Fig. 3), we observed a similar trend. NS4A colocalised with dsRNA in all samples, although the phenotype differed slightly in the more attenuated P48A and G66A samples (Fig. 3d–f and j–l). Interestingly, the dsRNA staining signal also did not vary dramatically despite the mutations made, indicating that only a small amount of NS4A (mutant or WT) was necessary for RC formation and dsRNA production. Overall, the combined data suggested that the mutations generated in NS4A did not prevent intracellular replication but did result in an overall decrease in efficiency.

Attenuated mutants show reduced intracellular membrane proliferation

It has been observed that proliferation of intracellular membranes coincides with the exponential increase in WNV_{KUN} replication (Ng and Hong, 1989), and that expression of NS4A alone is sufficient to induce CM/PC-like structures (Miller et al., 2007; Roosendaal et al., 2006).

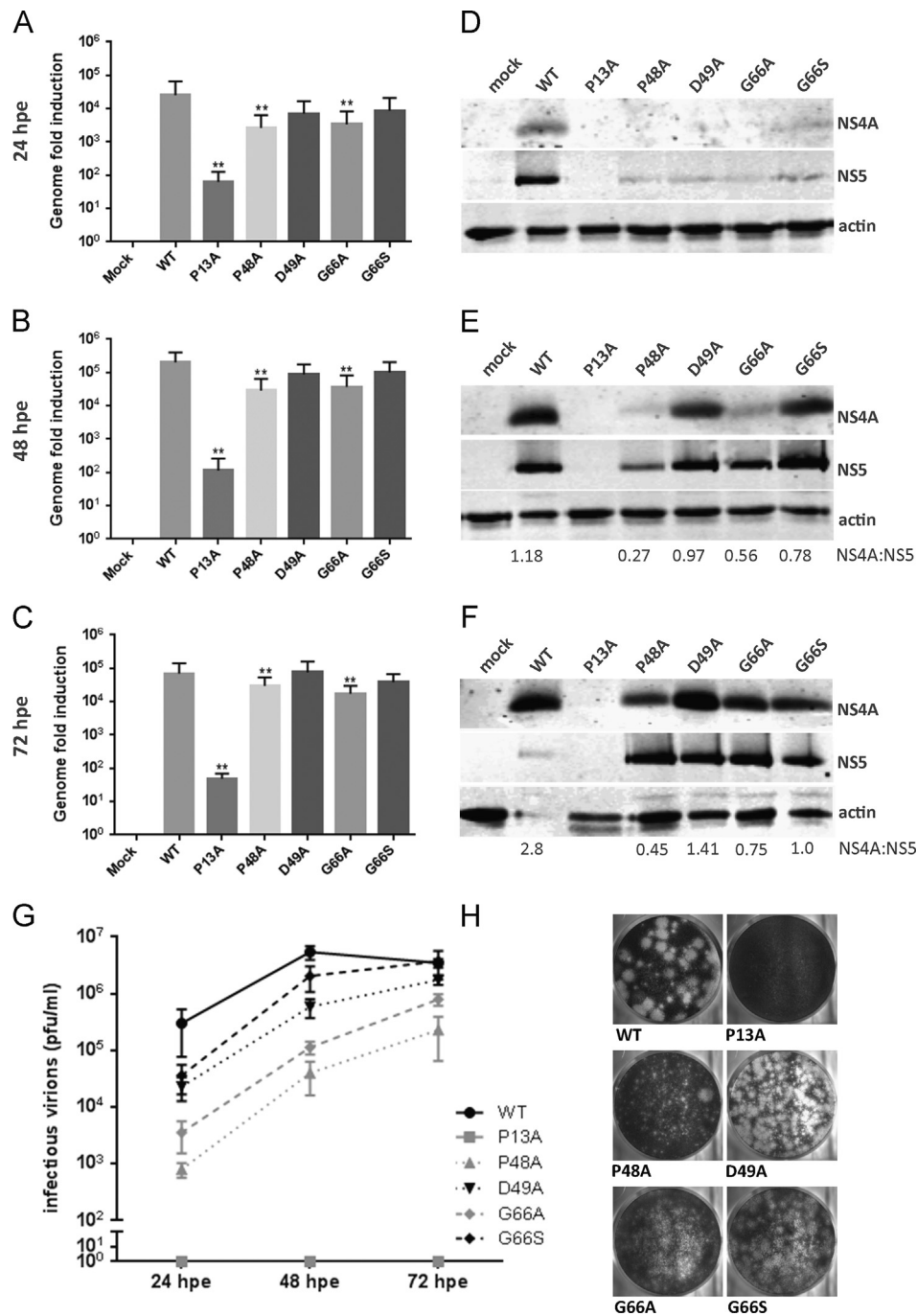


Fig. 1. N-terminal mutations in WNV_{KUN} NS4A differentially impair replication and virion production. Vero cells were electroporated with in-vitro synthesised FLSDX RNA and protein lysates and cell culture supernatants were collected at 24, 48 and 72 h.p.e. (A–C) RNA collected from the various samples was quantified for WNV_{KUN} genome levels using qPCR. Error bars indicate +1 standard deviation from triplicate experiments, and asterisks (**) indicate a significant change compared to WT FLSDX as determined by paired *t*-test (Graph Prism). (D–F) Protein lysates were analysed by western blot using antibodies raised against WNV_{KUN} proteins NS4A and NS5, and the internal control actin. Ratios shown were determined by densitometry analyses compared to actin. (G) Cell culture supernatants were analysed by plaque assay for infectious virion secretion and error bars (± 1 standard deviation) indicate duplicate analysis of triplicate experiments. (H) Visible plaques in the 10^{-5} dilution were analysed for size difference after staining with toluidine blue.

Thus, we were interested in determining if the mutations we generated in NS4A could also affect its ability to remodel intracellular membranes. To this end, we examined 50 nm thin sections from resin-embedded samples collected at 72 h.p.e. for membrane formation. As shown in Fig. 4, FLSDX WT-electroporated cells contained VPs as well as large areas of CM and PC and virions within vesicles were also observed (panels A and B). By visual comparison, the number and size of VPs in the N-terminal mutants did not vary considerably (Fig. 4, panels C–F),

which correlated with the dsRNA staining in the previous figure. However, the size of the CM/PC structures was radically reduced in the P48A and G66A mutants (Fig. 4, panels C and E); in particular, no CM/PC proliferations were detectable in any G66A-electroporated cells and very few were observed in the P48A samples. This data suggested that the overall decrease in NS4A protein levels in these mutants (Fig. 1D–F) was most likely preventing CM/PC formation. Additionally, the P48A mutant revealed large numbers of VP and virions (panel C),

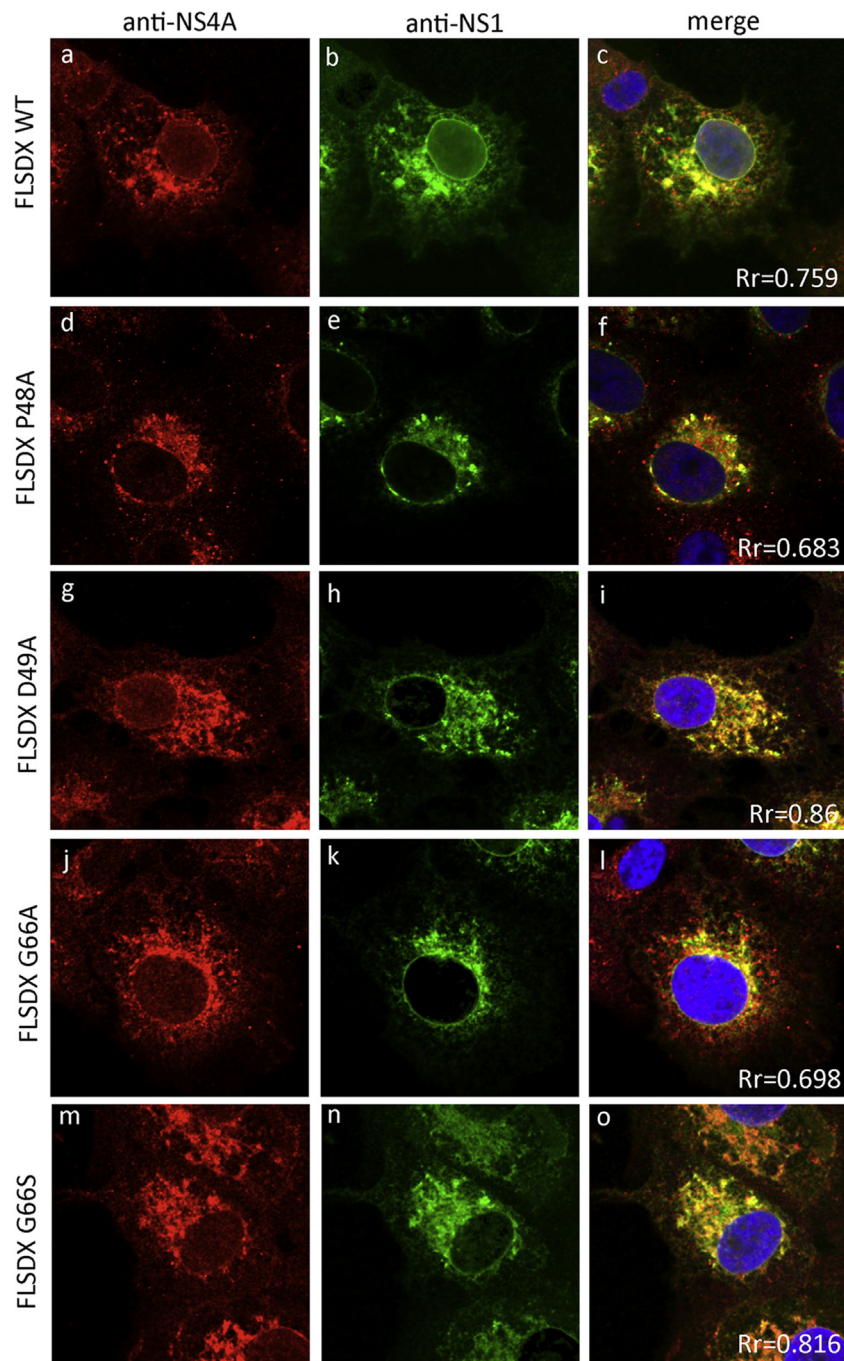


Fig. 2. N-terminal mutations decrease efficiency of replication but do not prevent replication complex formation. Vero cells were electroporated with in-vitro synthesised FLSDX RNA, fixed at 48 h.p.e. and labelled with antibodies to WNV_{KUN} NS4A (red) and NS1 (green). Nuclei were counterstained with DAPI. Pearson coefficient values (Rr) shown were computed using ImageJ.

implying that the majority of available NS4A was utilised for the formation of the RC and replication of the viral RNA.

Inhibition of proteasome-mediated degradation restores NS4A levels but does not restore RNA replication or virion secretion

We were intrigued by the decreased NS4A levels in the P48A and G66A samples (Fig. 1D–F), and hypothesised that the introduced mutations caused specific degradation of the mutant NS4A proteins, which would explain the discrepancies in NS4A:NS5 ratios. To address this, we harvested t.c.f. samples from electroporated Vero cells at 72 h. p.e. and re-infected Vero cells (m.o.i 0.1) with each of the mutant viruses for 24 h, then treated infected cells for a further 24 h with

inhibitors of the proteasomal (Bortezomib) and the lysosomal (Chloroquine) degradation pathways. We then assessed the levels of NS4A by western blotting, compared to NS5 and the loading control actin. As shown in Fig. 5A, treatment of cells with the 26S proteasome inhibitor Bortezomib significantly increased NS4A levels (compared to untreated) in all the mutant samples as well as WT. Concomitantly, NS5 levels did not overtly change, nor did the loading control actin, suggesting this effect was limited to NS4A. Interestingly, a similar proteasome inhibitor MG132 did not restore NS4A levels to that of Bortezomib (data not shown) suggesting that the mutations generated in NS4A resulted in increased targeting to the proteasome for ER-associated degradation. In comparison, the lysosomal inhibitor Chloroquine did not restore NS4A levels compared to untreated, suggesting

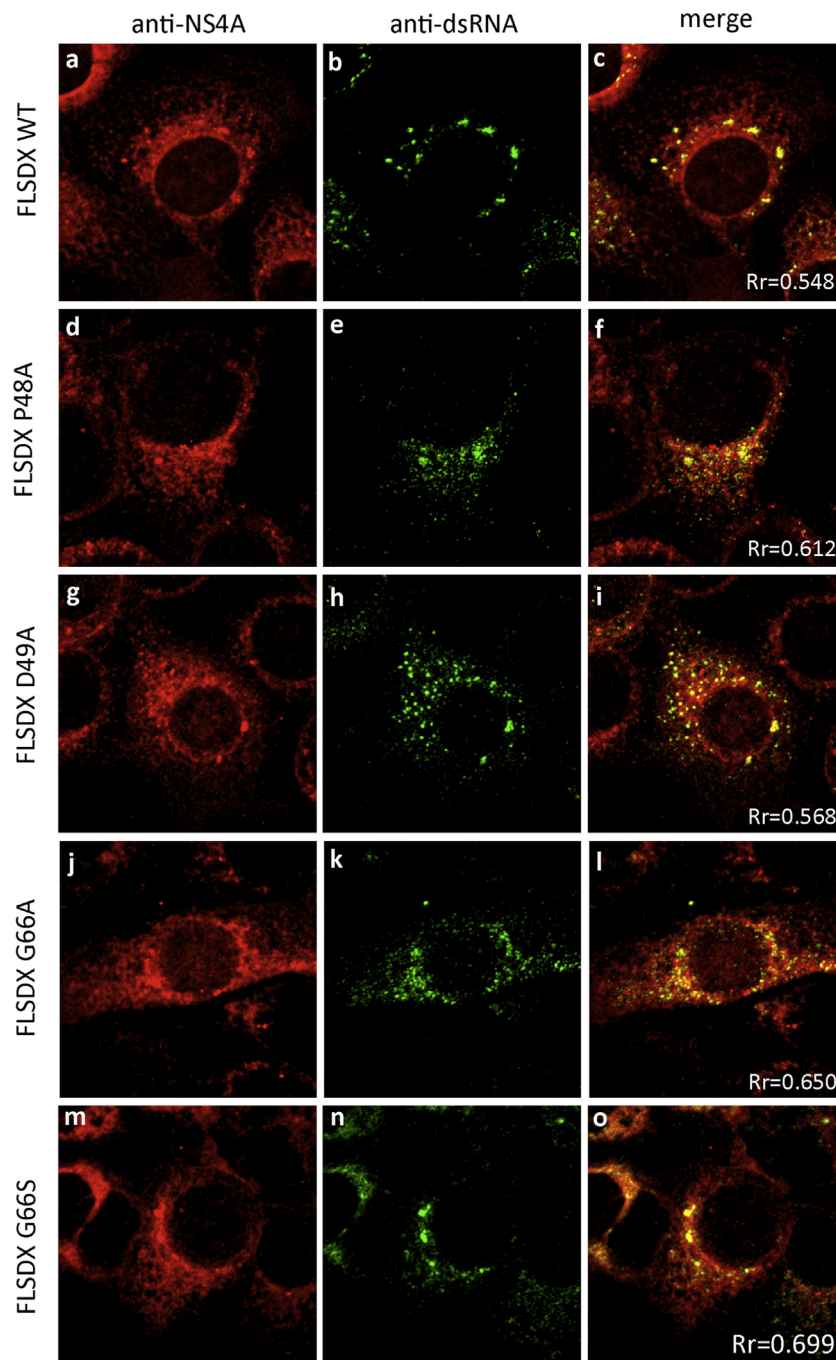


Fig. 3. N-terminal mutations decrease efficiency of replication but do not prevent replication complex formation. Vero cells were electroporated with in-vitro synthesised FLSDX RNA, fixed at 48 h.p.e. and labelled with antibodies to WNV_{KUN} NS4A (red) and the replicative intermediate dsRNA (green). Pearson coefficient values (R_r) shown were computed using ImageJ.

that the degradation of mutant NS4A was mediated by the proteasome. Intriguingly, we observed overall increases in WT as well as the mutant NS4A proteins. Overall however, the restoration in NS4A levels by Bortezomib was much more pronounced in the attenuated P48A and G66A mutants, supporting our hypothesis that these mutations are causing increased proteasomal degradation of NS4A and thus reducing membrane proliferation and efficiency of replication.

We next attempted to investigate whether the Bortezomib-mediated increases in NS4A levels could restore RNA replication and/or virion secretion. To assess this, we collected RNA and supernatants from re-infected cells treated with Bortezomib (or mock treated with DMSO) and assayed for genome replication via qPCR (Fig. 5B) and virus secretion by plaque assay (Fig. 5C). Intriguingly, we

did not observe any significant differences between Bortezomib and untreated samples with any of the WT or mutant viruses shown; overall, modest decreases were observed in all samples by qPCR and plaque assay analyses. Currently, we cannot completely explain the lack of effect of restoring NS4A has on WNV_{KUN} replication but suggest that the effect of Bortezomib may be contributing to the other functional roles of NS4A in modulating cellular and immune responses. These are areas we are currently investigating.

Bortezomib restoration in NS4A levels results in expansion of the ER

We were also interested in investigating whether the increased levels of NS4A in the attenuated mutants could rescue the ability of

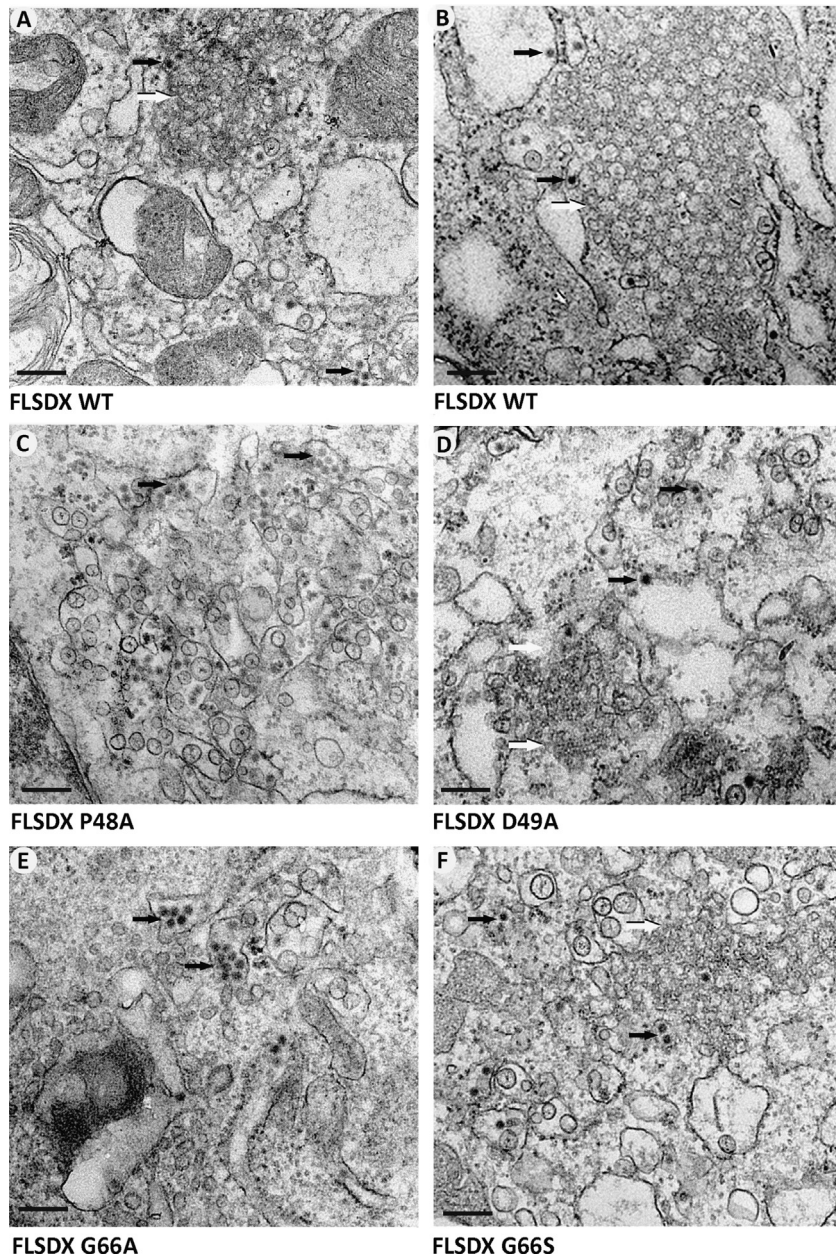


Fig. 4. Attenuated NS4A mutants show reduced intracellular membrane proliferation and ER recruitment. Vero cells were electroporated with in-vitro synthesised FLSDX RNA and fixed at 72 h.p.e. then processed for EM analysis. WNV_{KUN}-typical membrane structures paracrystalline arrays (PC) and convoluted membranes (CM) were observed as well as immature virions (black arrows). Black scale bar indicates 200 nM.

NS4A to remodel intracellular membranes. Thus, we compared NS4A, NS3 and dsRNA labelling in FLSDX WT, P48A and G66A-infected cells treated with Bortezomib (and untreated as a control). We observed that Bortezomib treatment caused increased thickening of the perinuclear region containing NS3, NS4A and dsRNA in all samples, including WT (arrows depict the thickened ER in Fig. 6). We proposed that this likely due to the increased proliferation of ER membranes, due to higher expression of both WT and mutant NS4A. To address this, we co-labelled infected cells with NS4A and NS3 as well as the resident ER protein, protein disulphide isomerase (PDI; Fig. 7). PDI has previously been shown to localise to WNV_{KUN}-induced membrane proliferations (Mackenzie and Westaway, 2001), and we observed significant colocalisation between NS3, NS4A and PDI in the Bortezomib-treated samples of FLSDX WT, P48A and G66A-infected cells (Fig. 7). In all the samples, there was an obvious increase in perinuclear staining of NS3 and NS4A (indicated by arrows) that colocalised with PDI (panels d, h, l, p, t and x). This was not apparent

in mock-infected cells treated with Bortezomib (Fig. 8), discounting the possibility that this thickening could be due to a non-specific effect of the proteasome inhibitor itself.

Discussion

Flavivirus NS4A is a highly conserved, ER-localised transmembrane protein with a number of functions in intracellular replication. We and others have investigated various conserved regions within this protein in order to further understand how it can perform its various roles in membrane proliferation, RC formation and regulation of cell signalling (Fig. 9) (Ambrose and Mackenzie, 2011a, b; Chang et al., 1999; Lin et al., 2008; Liu et al., 2005; McLean et al., 2011; Stern et al., 2013; Teo and Chu, 2014). Previously, we identified a conserved tetrapeptide motif in the C-terminal cytoplasmic loop responsible for correct proteolytic processing at the NS4A-2K site, which when mutated resulted in

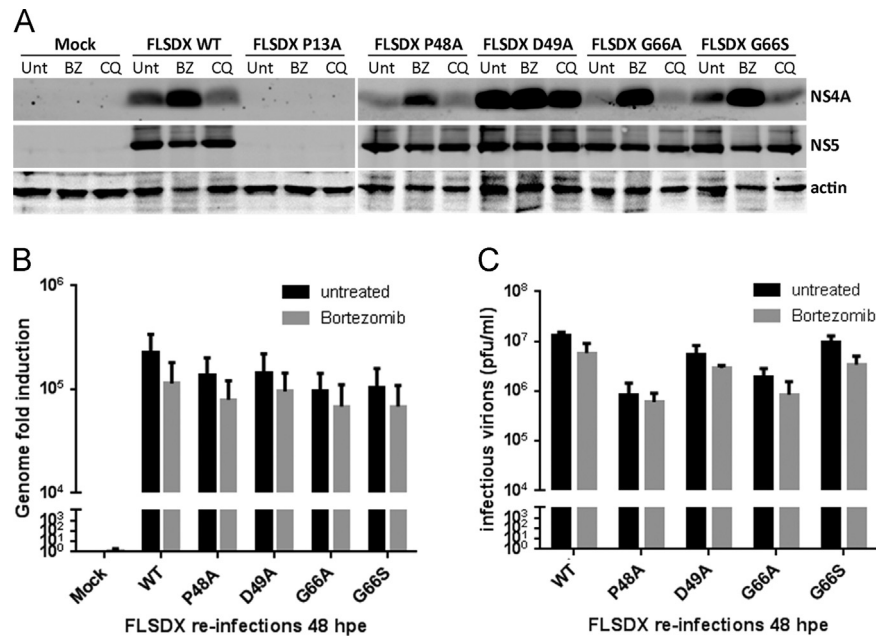


Fig. 5. Inhibition of proteasome-mediated degradation restores NS4A levels but does not improve RNA replication or virion production. Vero cells were infected at an m.o.i. of 0.1 with WT and mutant FLSDX viruses for 24 h, then treated with the chemical inhibitors (200 nM Bortezomib [BZ] or 1 μ M Chloroquine [CQ]) for a further 24 h. (A) Protein lysates were then collected and analysed by western blotting with antibodies to WNV_{KUN} NS4A and NS5 and the internal control actin. (B) RNA samples from mock, WT, P48A, D49A, G66A and G66S mock- or Bortezomib treated cells were analysed for WNV_{KUN} genome levels using qPCR. Error bars indicate +1 standard deviation of triplicate experiments. (C) Supernatant samples as above were analysed for infectious particle secretion by plaque assay. Error bars indicate +1 standard deviation of triplicate experiments.

complete ablation of WNV_{KUN} replication (Ambrose and Mackenzie, 2011a). To follow up on that study, we aimed to interrogate additional conserved regions in the N-terminus of WNV_{KUN} NS4A, which is proposed to interact with other replicase components and also mediate homodimerisation in DENV (Stern et al., 2013). Four conserved residues were selected for further study; Pro13 in the N-terminal cytoplasmic region, and Pro48, Asp49 and Gly66 associated with the first transmembrane helix (Fig. 9). These were mutated to alanine and/or serine within the WNV_{KUN} infectious clone, FLSDX, and assayed for effects on replication and intracellular membrane proliferation, which are two of the major functions of NS4A during WNV_{KUN} infection.

We observed that mutation of the cytoplasmic Pro13 to alanine (P13A) completely abolished WNV_{KUN} replication and virion secretion (Fig. 1). Perhaps this was not entirely unexpected; as NS4A is predicted to interact with replicase components (NS5, NS3 and replicating RNA) on the cytoplasmic face of the VP, it could be assumed that the hydrophilic N-terminal region would most likely mediate these associations. Thus, changes in this region could potentially have a deleterious effect on replicase associations and RC formation during early replication. Additionally, a recent study with DENV NS4A identified an amphipathic helix within the first 20 amino acids of the N-terminal region, which when disrupted reduced oligomerisation and completely abolished replication (Stern et al., 2013). Specific mutation of Pro13 to Ala within a DENV replicon also resulted in a replication null mutant. Interestingly, another study of DENV NS4A showed that the first 50 amino acids (corresponding to the cytoplasmic N-terminal region) could also interact with vimentin, a cellular protein associated with intermediate filaments. This association was proposed to be vital in the formation of DENV RCs (Teo and Chu, 2014), however we were unable to show any association of vimentin with the WNV RC (data not shown) implying there may be subtle differences in host component utilisation by the WNV and DENV. Overall, it could be proposed that the first 50 cytoplasmic residues of NS4A are vital for interaction with viral and cellular components, and mutations within this region (e.g. P13A) have a severe effect on RC formation and intracellular replication (Fig. 9).

The remaining mutations in the transmembrane region of WNV_{KUN} NS4A had variable effects on replication (Figs. 1 and 9). Two of the FLSDX mutants (P48A and G66A) were highly attenuated, with decreased viral protein synthesis and virion secretion, and also displayed significant defects in intracellular membrane proliferation. The remaining mutants (D49A and G66S) did show some early attenuation in protein and virus production, however at later time-points had similar levels of replication and an intracellular phenotype similar to WT. Interestingly, we observed a dramatic specific reduction in the levels of NS4A only in the highly attenuated mutants (Fig. 1A), implying a selective loss or degradation of mutant NS4A during replication. We proposed that the decreased NS4A levels could be attributed to proteasomal degradation, and attempted to rescue this by treating infected cells with inhibitors of both the lysosomal and proteasomal degradation pathways. Treatment with the 26S subunit inhibitor Bortezomib increased NS4A levels in all mutants as well as WT (Fig. 5), although the increase was much more pronounced in the P48A and G66A mutants. We suggest that these more severe mutations in or near the first transmembrane helix affected the folding and/or membrane insertion into the ER, and thus were targeted for ER-associated degradation. When we compared the effect of Bortezomib on the two Glycine mutations generated (non-conservative G66A vs. conservative G66S) it appeared to support a folding defect; the increase in G66A NS4A levels upon proteasome inhibition is much greater than in the equivalent G66S samples. Thus, maintaining helix associations with the serine substitution are resulting in a more stably-expressed protein and less attenuation at the level of virus replication. Of course we cannot discount that proteasome inhibitor, via BZ, may have other multiple consequences for virus replication, apart from increasing NS4A levels.

Our observation that Bortezomib treatment increased NS4A levels in WT, as well as mutant virus-infected cells is intriguing for multiple reasons. Given the hydrophobic nature of NS4A and its high levels of expression during replication, it could be proposed that a small proportion of WT NS4A could be targeted to the proteasome for

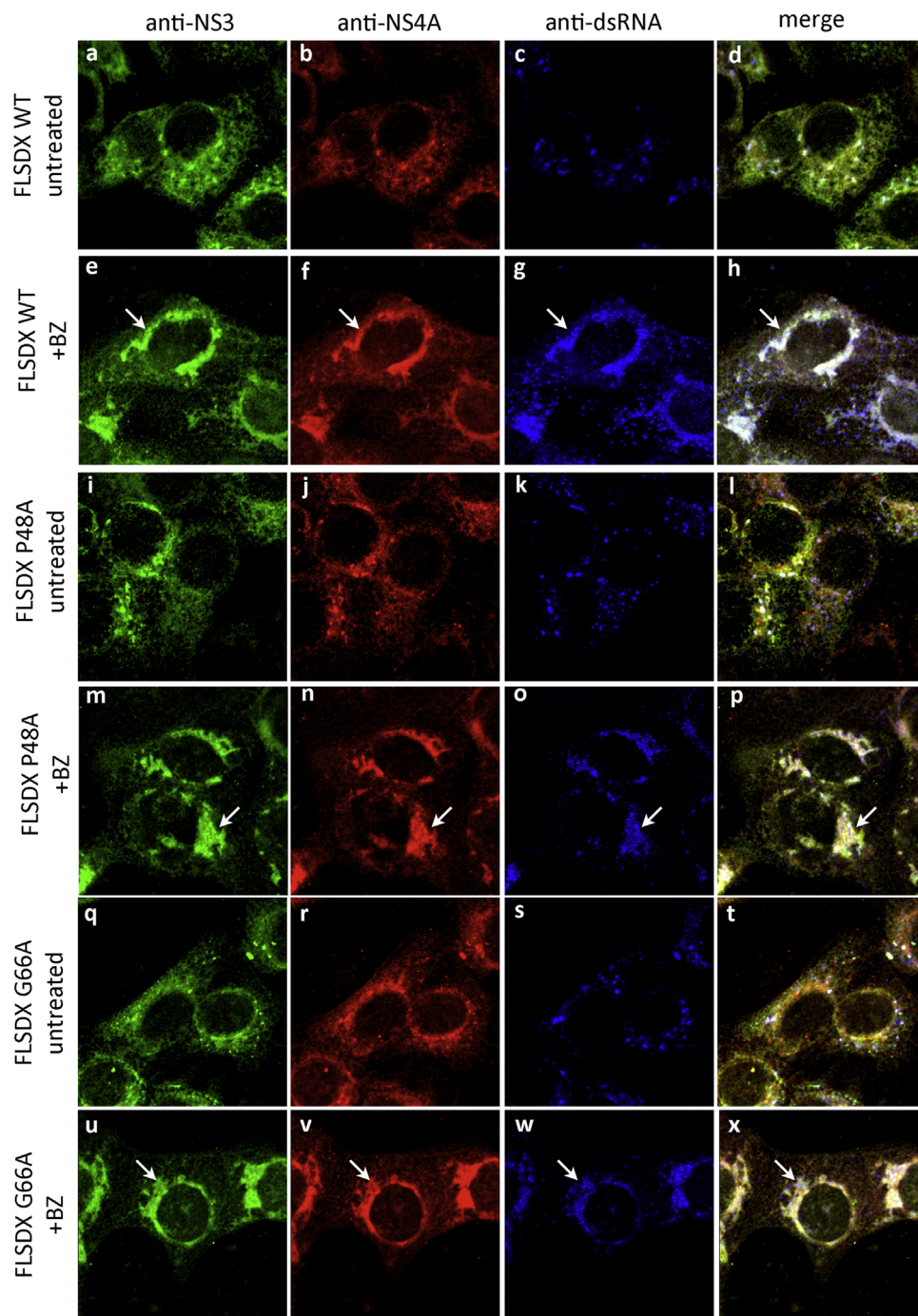


Fig. 6. Bortezomib restoration in NS4A levels results in expansion of the ER. Vero cells were infected at an m.o.i. of 0.1 with WT and mutant FLSDX viruses for 24 h, then treated with Bortezomib [BZ] for a further 24 h. Following fixation, cells were labelled with antibodies to WNV_{KUN} NS3 (green), NS4A (red) proteins and dsRNA (blue) and viewed on a Zeiss confocal microscope. Arrows depict the thickened ER after BZ treatment.

degradation, particularly oligomers. Additionally, we and others have shown that this very nature of NS4A is responsible for induction of UPR signalling, specifically IRE-1 and ATF6 activation (Ambrose and Mackenzie, 2011b), which are closely associated with ERAD via the proteasome as well as ER membrane biogenesis. Therefore, treatment with Bortezomib could also have partially restored all NS4A levels which may have originally been targeted for proteasomal degradation. Intriguingly, these overall increases in NS4A also caused a dramatic change to ER morphology in all the samples assayed, regardless of levels of replication (Fig. 7). Large perinuclear accumulations of NS4A and NS3 (both of which localise to the ER and ER-derived CM/PC structures) were observed, which also colocalised with the ER marker PDI. Thus we suggest that the increased levels of NS4A caused hyper-

proliferation of the ER, similar to what is observed upon over-expression of WNV_{KUN} NS4A alone (Roosendaal et al., 2006), that aids in the development of the viral RC to promote efficient replication. Our results would indicate that the levels of NS4A are important for replication most likely by contributing to membrane remodelling to compartmentalise the replicative components, including those for replication and assembly (Mackenzie and Westaway, 2001; Westaway et al., 1997a).

Overall, we propose that the replication defects associated with mutations in the first transmembrane region can be attributed to the misfolding and/or degradation of NS4A. The reduced protein levels of the P48A and G66A mutants were then insufficient for intracellular membrane proliferation and CM/PC formation, however, still

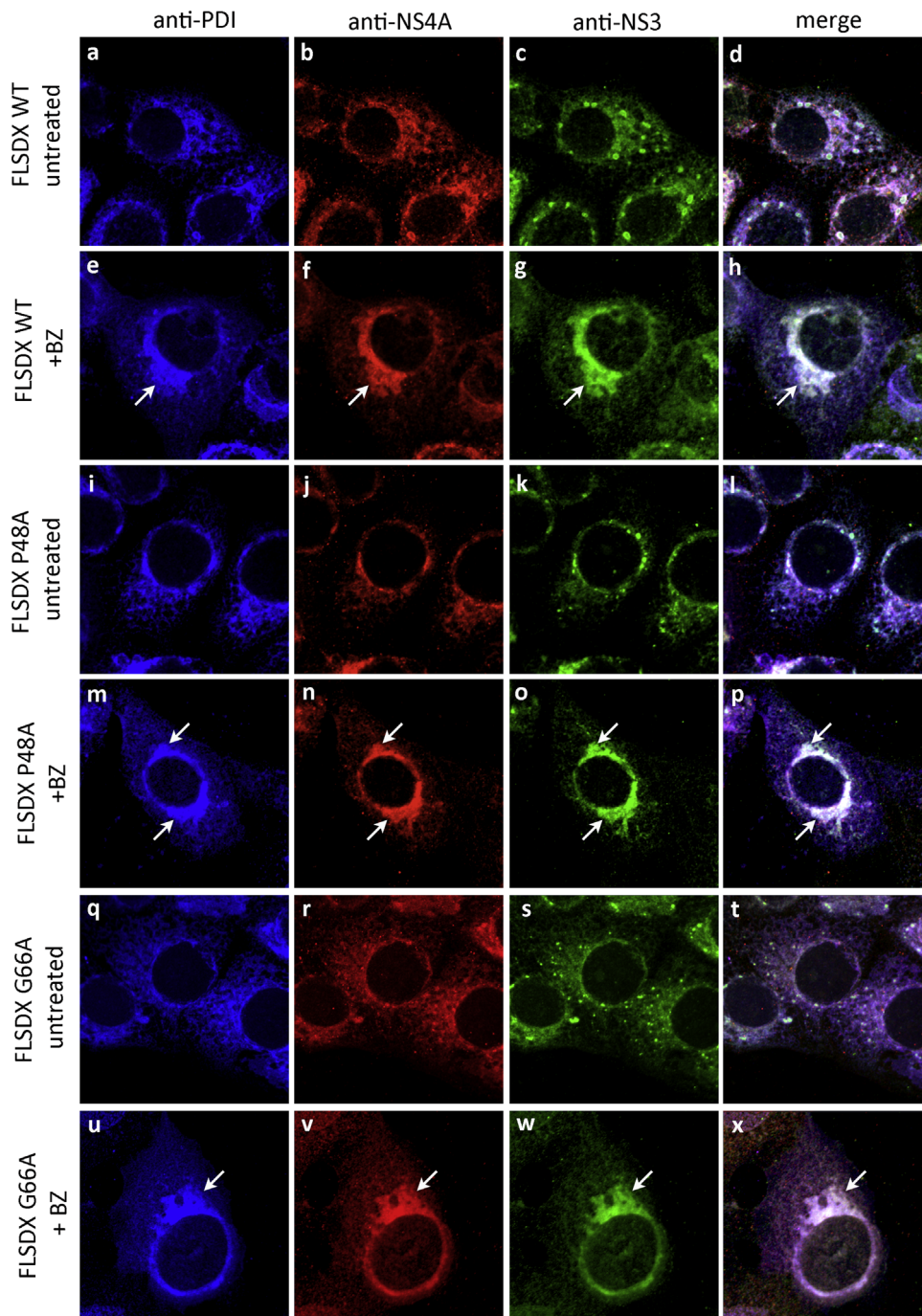


Fig. 7. Bortezomib restoration in NS4A levels results in expansion of the ER. Vero cells were infected at an m.o.i. of 0.1 with WT and mutant FLSDX viruses for 24 h, then treated with Bortezomib [BZ] for a further 24 h. Following fixation, cells were labelled with antibodies to WNV_{KUN} NS3 (green), NS4A (red) proteins and the host ER-resident protein Protein Disulphide Isomerase (PDI; blue) and viewed on a Zeiss confocal microscope.

permitted RC associations and RNA replication, as demonstrated by dsRNA staining. As the CM/PC structures are considered to be the sites of protein translation and proteolytic processing during WNV_{KUN} replication (Mackenzie, 2005; Westaway et al., 1997b), this may explain the decreased viral protein production at earlier timepoints in these mutants compared to WT and the less-attenuated D49A and G66A. As virion assembly also requires ER membranes, loss of ER proliferation could potentially reduce the levels of secreted virions, also observed in the more attenuated mutants.

In conclusion, we showed that mutations in the cytoplasmic region of WNV_{KUN} NS4A completely abolished replication, whilst changes to the first transmembrane helix caused increased degradation of NS4A

via the proteasome, which resulted in inefficient replication and loss of intracellular membrane proliferation. This data supports previous studies that have identified the cytoplasmic N-terminus of NS4A as a vital region for its function during replication. It also correlates with previous observations that only low levels of NS4A are required for RC associations and initiation of replication, however a higher, threshold level is needed to induce the proliferation of CM/PC structures, loss of which results in inefficient replication and virion secretion (Fig. 9A). Combining this information with our previous work on the proteolytic processing of NS4A, and other published data, we can now attribute specific regions of NS4A to functions during Flavivirus replication (Fig. 9B), and the relative importance of these roles. The N-terminal,

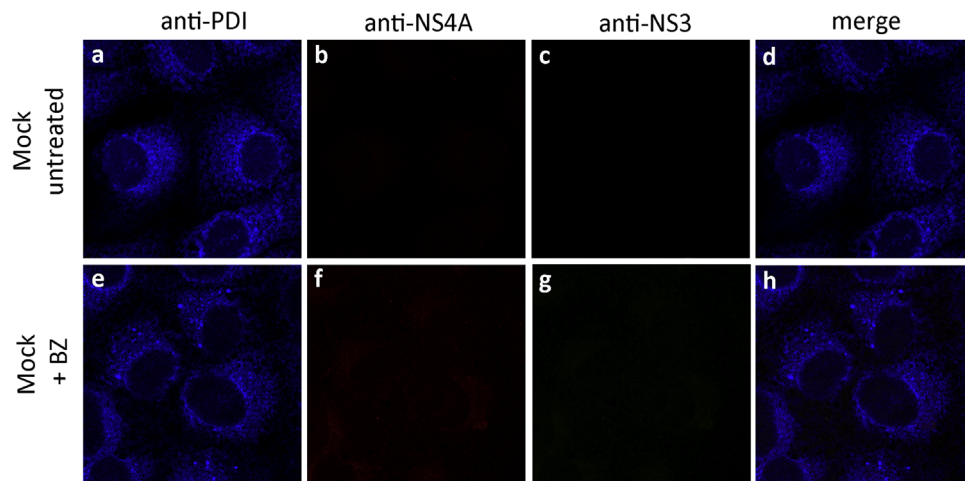


Fig. 8. Vero cells were mock-infected for 24 h, then treated with Bortezomib [BZ] for a further 24 h. Following fixation, cells were labelled with antibodies to WNV_{KUN} NS3 (green), NS4A (red) proteins and the host ER-resident protein Protein Disulphide Isomerase (PDI; blue) and viewed on a Zeiss confocal microscope.

A

Mutant	Replication	RC associations	Membrane induction	Protein degradation
WT	High	Y	Y	Y
P13A	None	N	ND	ND
P48A	Attenuated	Y	reduced	N
D49A	High	Y	Y	Y
G66A	Attenuated	Y	reduced	N
G66S	High	Y	Y	Y

B

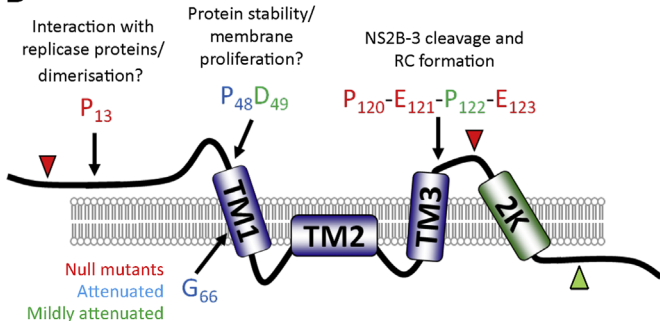


Fig. 9. Summary of current NS4A mutagenesis effects on WNV_{KUN} replication. Our current data investigating the effect of alanine/serine substitutions at various conserved residues of NS4A is summarised in Fig. 8. (A) The effect of these mutations on WNV_{KUN} replication, RC associations, membrane proliferation and NS4A protein levels is shown. Membrane induction and NS4A protein levels were not determined (ND) for the null mutation P13A. (B) The combined information from our studies into conserved regions of NS4A is shown in context with the predicted topology of NS4A within the ER membrane. Amino acids in red denote null mutants in FLSDX, blue residues indicate attenuated viruses and residues in green have little or no effect on WNV_{KUN} replication when mutated. Red arrows show dibasic cleavage sites targeted by the NS2B-3 protease whilst the black arrow indicates the signalase cleavage site. From this and other published studies we predict that the N-terminal region of NS4A is vital for protein–protein interactions between viral and cellular components, the first transmembrane region maintains protein stability and the final cytoplasmic loop is necessary for correct protease site presentation and cleavage by NS2B-3.

cytoplasmic region is crucial to replication, for the interaction with both viral and host components as well as oligomerisation. In comparison, the amino acids near and in the first transmembrane helix are important for protein stability and potentially membrane associations, which when mutated result in severe attenuation and NS4A degradation. Overall, this data provides more information about

the contributions of NS4A to Flavivirus replication and identifies regions associated with these functions, which could be used for antiviral targets in the future.

Materials and methods

Cells and antibodies

Vero cells were maintained in high-glucose DMEM (Life Technologies) supplemented with 5% Foetal Bovine Serum (FBS; Serum Supreme, Lonza), 50 U/mL–50 µg/mL Penicillin/Streptomycin (Gibco) and 200 mM Glutamax (Gibco). Mouse anti-NS5 and NS1 monoclonal antibodies were a kind gift from Prof Roy Hall (University of Queensland). WNV_{KUN}-specific rabbit anti-NS4A polyclonal antisera were kindly provided by Prof Alexander Khromykh (University of Queensland) (Mackenzie et al., 1998; Westaway et al., 1997a) and goat anti-NS3 polyclonal sera from Prof. Paul Young (University of Queensland). Mouse anti-dsRNA (clone J2) and mouse anti-actin antibodies were purchased from English & Scientific Consulting Bt. (Hungry) and Santa Cruz Biotechnology respectively. Mouse anti-PDI antibody was purchased from Abcam. Bortezomib and Chloroquine were sourced from Sigma-Aldrich.

Site-directed mutagenesis of WNV_{KUN} infectious clones and in vitro transcription/electroporation

Alanine/Serine mutations were generated in the WNV_{KUN} cDNA infectious clone, FLSDX using site-directed mutagenesis (Stratagene) (Khromykh et al., 1998) with the primers described in Supplementary Table 1. FLSDX clones were linearised by *XhoI* and DNA purified using phenol:chloroform extraction. RNA was transcribed from 0.5 µg of each linearised clone using SP6 RNA polymerase (New England Biolabs) and electroporated into Vero cells using the Neon electro-poration system (Life Technologies) (2 × 1150 V pulses, 20 ms pulse width, infinite resistance) in 100 µL tips. Cells were recovered in growth medium (2% FBS, 200 mM Glutamax) at room temperature for 5 min then plated out into 6- and 24-well plates. Cell lysates and tissue culture fluid (t.c.f) samples were collected at 24, 48 and 72 h post-electroporation (h.p.e).

Mutant virus propagation and titre determination

Tissue culture fluid (t.c.f) samples were collected from electro-porated cells and centrifuged at 5000 rpm for 5 min to pellet dead

cells and debris. Supernatants were then diluted 10-fold in DMEM (10^{-1} – 10^{-6}) and used to infect Vero cells previously seeded in DMEM complete media in 6-well plates. Cells were infected with 250 μ L of stock dilutions (in duplicate) and incubated at 37 °C for 60 min. 2 mL of a semi-solid overlay containing 0.3% w/v low-melting point agarose, 2.5% w/v FCS, P/S, Glx, HEPES and NaCO_3 was added to cells and solidified at 4 °C for 30 min. Cells were incubated at 37 °C for 4 days, fixed in 10% formalin (Sigma) for 1 h and stained in 0.4% crystal violet (with 20% v/v methanol and PBS) at RT for 1 h. Plaques were manually counted and plaque-forming units per ml (pfu/mL) calculated.

Immunofluorescence analysis

Cells were fixed with 4% w/v paraformaldehyde (PFA) in PBS at RT for 10 min, then permeabilised (in 4% PFA/PBS) with 0.1% w/v TritonX-100 at RT for 10 min. Cells were then quenched in 0.2 M Glycine at RT for 7 min, and blocked for 15 min in 1% bovine serum albumin (BSA)/PBS at RT. Following washes with PBS, cells were incubated with primary antibodies in 1% BSA/PBS for 1 h at RT. Cells were washed 4 times in 0.2% BSA/PBS then incubated with species specific secondary antibodies conjugated to either Alexa Fluor 647, 594 or 488 in 1% BSA/PBS at RT for 45 min. Cells were washed in 0.2% BSA/PBS, then PBS followed by 5 min incubation with 4 μ g/ml DAPI to counterstain the nuclei. Coverslips were mounted with Ultramount (Fronine) and immunofluorescent staining was visualised on a Zeiss confocal microscope (LSM 700) and figures assembled using Adobe Photoshop™.

Western blot analysis

Cells were washed once with PBS then lysed with SDS lysis buffer (0.1% SDS, 0.5 mM EDTA, 10 mM Tris pH8.0, 150 mM NaCl) containing protease inhibitors (Protease inhibitor cocktail III, Astral Scientific) and pipetted multiple times to reduce viscosity. Lysates were loaded on a 12% Tris-glycine polyacrylamide gel and separated at 100 V for 2 h. Separated proteins were transferred to Hi-Bond ECL nitrocellulose membrane (Amersham) at 100 V for 75 min and blocked at RT in 5% skim milk/TBS (Diploma) with 0.05% Tween (TBS-T). Following blocking, membranes were washed for 15 min in TBS-T then incubated overnight in primary antibodies diluted in 5% BSA/TBS-T at 4 °C. Membranes were washed in TBS-T three times then incubated with species-specific secondary antibodies conjugated to either Alexa Fluor 488 or 647 at RT for 2 h. Following two washes in TBS-T and one wash in TBS, membranes were viewed on the PharosFX fluorescent scanner (Bio-Rad). Densitometry analyses were performed using the Quantity One software (Bio-Rad) as indicated by manufacturers.

RNA extraction and qPCR analyses

Cells were lysed in Trizol Reagent (Life Technologies) and RNA extracted as indicated by the manufacturers. 1 μ g of total RNA was treated with RQ1 DNase (Promega) at 37 °C for 30 min to remove any contaminating cellular DNA, and cDNA generated with the Sensifast cDNA synthesis kit (Bioline) using both oligo d(T) primers and random hexamers. Gene-specific cDNAs were amplified using primers to the WNV_{KUN} genome and the internal control RPL13A (as previously published (Ambrose and Mackenzie, 2011b)) with ITaq Universal Sybr Green (Bio-Rad) on an MX3000 real-time PCR machine (Agilent). Fold induction of the WNV_{KUN} genome was calculated by comparing threshold cycle values (CT) to the internal control RPL13A.

Resin thin sections for electron microscopy

Cells were fixed with 3% w/v glutaraldehyde in 0.1 M cacodylate buffer for 2 h at room temperature. Cells were then washed several times in 0.1 M cacodylate buffer followed by fixation with 1% OsO₄ in

0.1 M cacodylate buffer for 1 h. After washing of the cells in 0.1 M cacodylate buffer, specimens were dehydrated in graded acetones for 10–20 min each. Subsequently, samples were infiltrated with EPON resin and polymerised in moulds for 2 days at 60 °C. 50 nm thin sections were cut on a Leica UC7 ultramicrotome using a Diatome diamond knife and collected on formvar and carbon-coated copper mesh grids. Before viewing in TF30 transmission electron microscope cells were post-stained with 2% aqueous uranyl acetate (UA) and Reynold's lead citrate.

Acknowledgments

We thank Alexander Khromykh, Roy Hall and Paul Young for generously providing the WNV_{KUN} infectious clones and replicons, and antibodies. We also acknowledge the assistance of Dr Eric Hanssen at the Advanced Microscopy facility, Bio21 Institute, University of Melbourne. This research was partially supported by a Project Grant (no. 1004619) to J.M. from the National Health and Medical Research Council of Australia.

Appendix A. Supporting information

Supplementary data associated with this article can be found in the online version at <http://dx.doi.org/10.1016/j.virol.2015.02.045>.

References

- Ambrose, R.L., Mackenzie, J.M., 2011a. A conserved peptide in West Nile virus NS4A protein contributes to proteolytic processing and is essential for replication. *J. Virol.* 85, 11274–11282.
- Ambrose, R.L., Mackenzie, J.M., 2011b. West Nile virus differentially modulates the unfolded protein response to facilitate replication and immune evasion. *J. Virol.* 85, 2723–2732.
- Chang, Y.S., Liao, C.L., Tsao, C.H., Chen, M.C., Liu, G.L., Chen, L.K., Lin, Y.L., 1999. Membrane permeabilization by small hydrophobic nonstructural proteins of Japanese encephalitis virus. *J. Virol.* 73, 6257–6264.
- Chu, P.W.G., Westaway, E.G., 1992. Molecular and ultrastructural analysis of heavy membrane fractions associated with the replication of Kunjin virus RNA. *Arch. Virol.* 125, 177–191.
- Egger, D., Wolk, B., Gosert, R., Bianchi, L., Blum, H.E., Moradpour, D., Bienz, K., 2002. Expression of hepatitis C virus proteins induces distinct membrane alterations including a candidate viral replication complex. *J. Virol.* 76, 5974–5984.
- Gillespie, L.K., Hoenen, A., Morgan, G., Mackenzie, J.M., 2010. The endoplasmic reticulum provides the membrane platform for biogenesis of the flavivirus replication complex. *J. Virol.* 84, 10438–10447.
- Khromykh, A.A., Kenney, M.T., Westaway, E.G., 1998. Trans-complementation of flavivirus RNA polymerase gene NS5 by using Kunjin virus replicon-expressing BHK cells. *J. Virol.* 72, 7270–7279.
- Lin, C.W., Cheng, C.W., Yang, T.C., Li, S.W., Cheng, M.H., Wan, L., Lin, Y.J., Lai, C.H., Lin, W.Y., Kao, M.C., 2008. Interferon antagonist function of Japanese encephalitis virus NS4A and its interaction with DEAD-box RNA helicase DDX42. *Virus Res.* 137, 49–55.
- Liu, W.J., Wang, X.J., Mokhonov, V.V., Shi, P.Y., Randall, R., Khromykh, A.A., 2005. Inhibition of interferon signaling by the New York 99 strain and Kunjin subtype of West Nile virus involves blockage of STAT1 and STAT2 activation by nonstructural proteins. *J. Virol.* 79, 1934–1942.
- Mackenzie, J., 2005. Wrapping things up about virus RNA replication. *Traffic* 6, 967–977.
- Mackenzie, J.M., Khromykh, A.A., Jones, M.K., Westaway, E.G., 1998. Subcellular localization and some biochemical properties of the flavivirus Kunjin nonstructural proteins NS2A and NS4A. *Virology* 245, 203–215.
- Mackenzie, J.M., Khromykh, A.A., Westaway, E.G., 2001. Stable expression of noncytopathic Kunjin replicons simulates both ultrastructural and biochemical characteristics observed during replication of Kunjin virus. *Virology* 279, 161–172.
- Mackenzie, J.M., Westaway, E.G., 2001. Assembly and maturation of the flavivirus Kunjin virus appear to occur in the rough endoplasmic reticulum and along the secretory pathway, respectively. *J. Virol.* 75, 10787–10799.
- McLean, J.E., Wudzinska, A., Datan, E., Quaglino, D., Zakeri, Z., 2011. Flavivirus NS4A-induced autophagy protects cells against death and enhances virus replication. *J. Biol. Chem.* 286, 22147–22159.
- Miller, S., Kastner, S., Krijnse-Locker, J., Buhler, S., Bartenschlager, R., 2007. The non-structural protein 4A of dengue virus is an integral membrane protein inducing membrane alterations in a 2K-regulated manner. *J. Biol. Chem.* 282, 8873–8882.

- Munoz-Jordan, J.L., Sanchez-Burgos, G.G., Laurent-Rolle, M., Garcia-Sastre, A., 2003. Inhibition of interferon signaling by dengue virus. In: *Proceedings of the National Academy of Sciences of the United States of America* 100, pp. 14333–14338.
- Ng, M.L., Hong, S.S., 1989. Flavivirus infection - essential ultrastructural changes and association of Kunjin virus NS3 protein with microtubules. *Arch. Virol.* 106, 103–120.
- Roosendaal, J., Westaway, E.G., Khromykh, A., Mackenzie, J.M., 2006. Regulated cleavages at the West Nile virus NS4A-2K-NS4B junctions play a major role in rearranging cytoplasmic membranes and golgi trafficking of the NS4A protein. *J. Virol.* 80, 4623–4632.
- Stern, O., Hung, Y.F., Valdau, O., Yaffe, Y., Harris, E., Hoffmann, S., Willbold, D., Sklan, E.H., 2013. An N-terminal amphipathic helix in dengue virus nonstructural protein 4A mediates oligomerization and is essential for replication. *J. Virol.* 87, 4080–4085.
- Teo, C.S.H., Chu, J.J.H., 2014. Cellular vimentin regulates construction of dengue virus replication complexes through interaction with NS4A protein. *J. Virol.* 88, 1897–1913.
- Westaway, E.G., Mackenzie, J.M., Kenney, M.T., Jones, M.K., Khromykh, A.A., 1997a. Ultrastructure of Kunjin virus-infected cells: colocalization of NS1 and NS3 with double-stranded RNA, and of NS2B with NS3, in virus-induced membrane structures. *J. Virol.* 71, 6650–6661.
- Westaway, E.G., MacKenzie, J.M., Kenney, M.T., Jones, M.K., Khromykh, A.A., 1997b. Ultrastructure of Kunjin virus-infected cells: colocalization of NS1 and NS3 with double-stranded RNA, and of NS2B with NS3, in virus-induced membrane structures. *J. Virol.* 71, 6650–6661.
- Westaway, E.G., Mackenzie, J.M., Khromykh, A.A., 2002. Replication and gene function in Kunjin virus, Japanese encephalitis and West Nile viruses. Springer-Verlag Berlin, Berlin, pp. 323–351.